

Consequences of a Rare Complement Factor H Variant for Age-Related Macular Degeneration in the Amish

Andrea R. Waksmunski,¹⁻³ Kristy Miskimen,³ Yeunjoo E. Song,³ Michelle Grunin,^{2,3} Renee Laux,³ Denise Fuzzell,³ Sarada Fuzzell,³ Larry D. Adams,⁴ Laura Caywood,⁴ Michael Prough,⁴ Dwight Stambolian,⁵ William K. Scott,⁴ Margaret A. Pericak-Vance,⁴ and Jonathan L. Haines¹⁻³

¹Department of Genetics and Genome Sciences, Case Western Reserve University, Cleveland, Ohio, United States

²Cleveland Institute for Computational Biology, Case Western Reserve University, Cleveland, Ohio, United States

³Department of Population and Quantitative Health Sciences, Case Western Reserve University, Cleveland, Ohio, United States

⁴John P. Hussman Institute for Human Genomics, University of Miami Miller School of Medicine, Miami, Florida, United States

⁵Department of Ophthalmology, University of Pennsylvania, Philadelphia, Pennsylvania, United States

Correspondence: Jonathan L. Haines, Department of Population and Quantitative Health Sciences, Case Western Reserve University, 10900 Euclid Avenue, Cleveland, OH 44106-7020, USA; jlh213@case.edu.

Received: November 9, 2021

Accepted: July 12, 2022

Published: August 5, 2022

Citation: Waksmunski AR, Miskimen K, Song YE, et al. Consequences of a rare complement factor H variant for age-related macular degeneration in the Amish. *Invest Ophthalmol Vis Sci.* 2022;63(9):8. <https://doi.org/10.1167/iovs.63.9.8>

PURPOSE. Genetic variants in the complement factor H gene (*CFH*) have been consistently implicated in age-related macular degeneration (AMD) risk. However, their functional effects are not fully characterized. We previously identified a rare, AMD-associated variant in *CFH* (P503A, rs570523689) in 19 Amish individuals, but its functional consequences were not investigated.

METHODS. We performed genotyping for *CFH* P503A in 1326 Amish individuals to identify additional risk allele carriers. We examined differences for age at AMD diagnosis between carriers and noncarriers. In blood samples from risk allele carriers and noncarriers, we quantified (i) *CFH* RNA expression, (ii) CFH protein expression, and (iii) C-reactive protein (CRP) expression. Potential changes to the CFH protein structure were interrogated computationally with Phyre² and Chimera software programs.

RESULTS. We identified 39 additional carriers from Amish communities in Ohio and Indiana. On average, carriers were younger than noncarriers at AMD diagnosis, but this difference was not significant. *CFH* transcript and protein levels in blood samples from Amish carriers and noncarriers were also not significantly different. CRP levels were also comparable in plasma samples from carriers and noncarriers. Computational protein modeling showed slight changes in the CFH protein conformation that were predicted to alter interactions between the CFH 503 residue and other neighboring residues.

CONCLUSIONS. In total, we have identified 58 risk allele carriers for *CFH* P503A in the Ohio and Indiana Amish. Although we did not detect significant differences in age at AMD diagnosis or expression levels of CFH in blood samples from carriers and noncarriers, we observed modest structural changes to the CFH protein through *in silico* modeling. Based on our functional and computational observations, we hypothesize that *CFH* P503A may affect CFH binding or function rather than expression, which would require additional research to confirm.

Keywords: age-related macular degeneration, complement factor H, rare variant, protein structure

Age-related macular degeneration (AMD) is among the leading causes of irreversible vision loss in the world.¹ Individuals with AMD experience a loss of central vision as the disease progresses with drusen accumulation, photoreceptor death, and neovascularization in the macula.² The results of family and twin studies demonstrated that there is a strong genetic component to AMD risk.³⁻¹⁰ Genomewide association studies (GWAS) performed by the International AMD Genomics Consortium (IAMDC) identified 52 common and rare genomic variants associated with AMD in the general population of European descent.¹¹ Additional

risk variants, including rare variants, have been associated with AMD.¹²⁻¹⁴ Although these studies uncovered genetic variation that plays a role in AMD risk and development, they do not necessarily interrogate the biological consequences of these genetic changes. Moreover, the results from these studies have highlighted the need for functional studies to characterize the biological effects of these variants.

Variants in the complement factor H (*CFH*) gene were among the first AMD-associated variants identified through GWAS¹⁵⁻¹⁷ and have been repeatedly associated with AMD risk in the general population.¹¹ Perturbations in the CFH

protein are suspected to alter both systemic and local complement regulation and promote immune responses in the retina that contribute to AMD.^{18–20} Despite this, the biological implications of these variants are not fully understood, and the development of effective complement-based therapies have remained mostly unsuccessful.^{21,22}

We previously identified a rare, missense variant in *CFH* that was significantly associated with AMD in the Amish.¹³ Studying this population isolate offers a distinct opportunity to identify and study novel AMD variants because the Amish are more environmentally and genetically homogeneous than the general population of European descent.²³ In our previous study, we observed an Amish nuclear family in Ohio comprised of several AMD-affected family members that lacked the risk allele for the common *CFH* Y402H AMD-associated variant.¹³ Therefore, we performed whole exome sequencing of these individuals and subsequently identified *CFH* P503A (rs570523689) as a rare, risk variant for AMD ($P = 9.27 \times 10^{-13}$).¹³ The risk allele for this variant was identified in 19 Amish individuals (12 affected, 5 unaffected, and 2 unknown AMD status) and was computationally predicted to be damaging to the CFH protein structure and function.¹³ However, the functional effects of this variant were not examined.

The purpose of this study was to elucidate the functional consequences of *CFH* P503A in the Amish, which might inspire testable hypotheses for AMD etiology and development of therapeutics that could improve the lives of patients with AMD. We hypothesize that rare variants, in particular, may reveal insights into disease etiology and may be an effective target for therapeutic intervention because they are often expected to be damaging to the protein structure and to perturb cellular processes.

METHODS

Study Demographics

The participants for this study were recruited from Amish communities in Ohio, Indiana, and Pennsylvania as a part of the Collaborative Aging and Memory Project (CAMP)¹³ and Amish Eye Study.²⁴ Individuals were at least 50 years old and reported having at least one close relative with a diagnosis of AMD. Informed consent was acquired from all study subjects in accordance with the tenets of the Declaration of Helsinki. Clinical data and biological materials (samples) from study participants were collected under institutional review board (IRB)-approved protocols. AMD affection status was based on self-reported AMD diagnosis and clinically confirmed diagnoses from eye examinations performed at each respective clinical center (Ohio, Indiana, and Pennsylvania) where ocular coherence tomography (OCT) images were obtained for both eyes. We previously found that, in the Amish, the positive and negative predictive values for self-reported AMD diagnosis compared to clinical diagnoses were 89% and 90%, respectively.¹³ From the OCT images, each eye was graded based on a modified Clinical Age-Related Maculopathy Staging (CARMS) system.^{25,26} Individuals with a grade of 3 or higher in at least one eye were considered AMD-affected. Individuals with grades of 2 or lower in both eyes were considered unaffected.

Blood Collection

Peripheral blood was collected from study participants via intravenous methods under IRB-approved protocols. We

collected whole blood for DNA extraction and white blood cells for protein lysates using Vacutainer EDTA Tubes (BD). Plasma was collected by spinning whole blood from EDTA tubes at $2500 \times g$ for 10 minutes. Whole blood for RNA extraction was collected in PAXgene Blood RNA Tubes (Qiagen).

Nucleic Acid Extraction

Genomic DNA was extracted from 1 mL whole blood aliquots using QIASymphony DSP DNA Kit (Qiagen) on a QIASymphony SP automated system (Qiagen). DNA concentration and 260/280 ratio were determined using a NanoDrop Spectrophotometer (Thermo Fisher). DNA integrity was confirmed using an e-Gel Precast Agarose Electrophoresis System (Thermo Fisher) using a 1% agarose gel. RNA was extracted from PAXgene Blood RNA Tubes using the QIASymphony PAXgene Blood RNA Kit (Qiagen) on a QIASymphony automated system. RNA concentration and 260/280 ratio for quality control were determined using a NanoDrop Spectrophotometer.

P503A Genotyping

We performed custom TaqMan genotyping assays (Thermo Fisher) following the manufacturer's instructions using 12.5 ng of genomic DNA per reaction and TaqMan Genotyping Master Mix (Thermo Fisher). Our assays utilized custom probes for the *CFH* P503A variant that assessed the presence of the C allele (non-risk, P503) compared to the G allele (risk, A503) at position 1507 in the *CFH* transcript. The forward primer sequence of the probe is AATTACATGTGGGAAAGATGGATGGT. The reverse primer sequence of the probe is CTTTGTGTATCATCTGGATAATCAATACAAACAT. Each 96-well plate included at least one known carrier of the risk allele for *CFH* P503A as controls. Blanks were also included on each plate. The assays were run on a QuantStudio 7 PCR instrument and performed genotype calling with the QuantStudio analysis software.

Amish Pedigrees

Using data from the Anabaptist Genealogy Database (AGDB),²⁷ we constructed both all-connecting path (ACP) and all-shortest path (ASP) pedigrees for the 58 Amish carriers of the risk allele, which included the 19 previously identified carriers¹³ and the 39 newly identified carriers. An ACP pedigree depicts all possible familial relationships among persons of interest in the pedigree. An ASP pedigree shows the closest relationships among these individuals. The ACP pedigree was visualized using Pedigraph.²⁸

We also constructed an ACP pedigree using data on the 1065 individuals in our study cohort who were genotyped for *CFH* P503A and had AMD diagnosis data. This pedigree information was used in our association analyses for kinship information.

Association Tests

Previous work identified *CFH* P503A as an AMD risk variant ($P = 9.27 \times 10^{-13}$) using the modified quasi-likelihood score (MQLS) software.¹³ Using our updated dataset, which included 224 AMD-affected individuals (93 from Ohio, 38 from Indiana, and 93 from Pennsylvania) and 841 unaffected individuals (250 from Ohio, 220 from Indiana, and 371 from Pennsylvania), we performed association tests for

CFH P503A and AMD status using both unadjusted and covariate-adjusted (age, sex, and Amish community location) analyses with a generalized linear mixed model accounting for familial relatedness. We generated kinship matrices using the kinship2 R package²⁹ based on (i) the immediate pedigree relationships of the 1065 genotyped individuals in our datasets (i.e. sibship-based kinship matrix) and (ii) the full 5709-person ACP connecting these 1065 individuals (i.e. ACP-based kinship matrix).

Of the 1065 Amish individuals in our association analyses (50 carriers and 1015 noncarriers; and 224 AMD-affected and 841 unaffected), 59 individuals were included in the original association test described in Hoffman et al. 2014.¹³ This included 18 risk allele carriers (1 homozygote and 17 heterozygotes; and 12 AMD-affected and 6 unaffected) and 41 noncarriers of the risk allele (15 AMD-affected and 26 unaffected). Therefore, most of the originally published risk allele carriers (18 out of 19) were included in our association tests, but they did not comprise the majority of risk allele carriers in the analyses (18 out of 50). To determine if the originally identified *CFH* P503A risk allele carriers strongly contributed to the association signal in our updated analyses, we re-performed our association analyses with data from only the newly ascertained study participants, which included 1006 genotyped individuals of whom 197 were AMD-affected (73 from Ohio, 31 from Indiana, and 93 from Pennsylvania) and 809 were unaffected (222 from Ohio, 216 from Indiana, and 371 from Pennsylvania).

Age at Diagnosis

To determine if *CFH* P503A carrier status has implications for the age at onset for AMD, we examined the ages of the carriers and noncarriers when they received their first AMD diagnosis. This measurement served as a proxy for age of onset of AMD. We compared the ages using a Kaplan-Meier survival curve analysis in R between the carriers ($n = 31$) and noncarriers ($n = 795$). We also used a Wilcoxon rank-sum test to evaluate significant differences among carriers and noncarriers with and without AMD.

CFH RNA Quantification and Analysis

We examined mRNA expression of *CFH* in whole blood samples from 7 AMD-affected carriers, 14 unaffected carriers, 5 AMD-affected noncarriers, and 14 unaffected noncarriers. We performed assays targeting the three protein-coding transcripts of *CFH* (CFH-201, 202, and 206) and the large retained intron of *CFH* (CFH-203). First-strand cDNA synthesis was carried out using the SuperScript VILO cDNA Synthesis Kit (Invitrogen) on 500 ng of total RNA. For the real-time PCR, commercially available TaqMan Gene Expression Assays for *CFH* (*Hs00962360_m1*, *Hs00962373_m1*, and *Hs00962376_m1*) were used to quantify CFH-202 and the other protein-coding transcripts of *CFH* (CFH-201 and CFH-206). A Custom Plus TaqMan RNA Assay was designed to target CFH-203 (ARFVKWR). Commercially available assays for ACTB (*Hs99999903_m1*) and TBP (*Hs00427621_m1*) were also used for real-time PCR. Assays were prepared using the TaqMan Fast Advanced Master Mix (Thermo Fisher) and run on a QuantStudio 7 PCR instrument. Expression levels of each mRNA transcript were determined using the $2^{-\Delta\Delta Ct}$ method and normalized to ACTB or TBP endogenous control genes. We used TBP as the control gene in experiments using the custom assay designed to

target CFH-203 and the commercially available TaqMan Gene Expression Assay targeting the CFH-202 transcript alone (*Hs00962360_m1*). For the other two assays, we used ACTB as the control gene in our experiments. Expression of *CFH* in the Amish blood samples was quantified relative to the expression measured for ARPE-19 cells in the same assays. Pancreatic and liver cells were included in our assays as controls.

Quantitative analysis was performed using Microsoft Excel, and relative CFH transcript expression values were compared between groups (carrier versus noncarrier; and AMD versus non-AMD) using two-sided *t*-tests assuming unequal variances for each assay. We also evaluated differences among relative *CFH* transcript expression levels from carriers and noncarriers with and without AMD using Wilcoxon rank-sum tests between group pairs and using Kruskal-Wallis tests among all groups in each assay. Four outliers were removed from our analyses because they fell outside 1.5 times the interquartile range (IQR) of at least one of the assays we performed in this study. Therefore, our statistical tests were based on relative expression data from 6 AMD-affected carriers, 12 unaffected carriers, 5 AMD-affected noncarriers, and 13 unaffected noncarriers.

Western Blots and Quantitative Analysis

Plasma samples from study participants were diluted 1:10 in phosphate buffered saline (PBS). We added 1 μ L of diluted plasma to radioimmunoprecipitation assay (RIPA) buffer (ThermoFisher). Laemmli Sample Buffer (BioRad) containing β -mercaptoethanol was added to a final concentration of 1X. Samples were denatured at 100°C for 10 minutes and run on Novex WedgeWell 4-20% Tris-Glycine gels (Invitrogen). We ran 5 μ g of human liver whole tissue lysate (Novus Biologicals) on each gel as a control for CFH and C-reactive protein (CRP) expression. Separated proteins were transferred to polyvinylidene difluoride (PVDF) membranes (Thermo Fisher) and probed for CFH (Abcam ab8842 sheep polyclonal) or CRP (Abcam ab50861 mouse monoclonal). A rabbit anti-sheep secondary antibody conjugated to HRP was used for detection (Abcam ab6747). Signal was detected using ECL Solution (Advansta), and digital images were captured via the Odyssey Imaging System (LI-COR). Complete transfer and equal protein loading were confirmed using the Novex Reversible Membrane Protein Stain Kit (Thermo Fisher).

Quantitative analyses were performed using ImageJ³⁰ and the following protocol.³¹ Briefly, blot photographs were transformed into 8-bit grayscale photographs, and all measurements were taken in “grey mean value” values. An area to examine was set based on the largest possible band size, and the identical examination/selection area was used for every band per blot and every background per blot. Background measurement was taken from the blank area on the blot above each band. Measurements were inverted relative to their pixel density (i.e. 255 minus the measurement taken). Matched background was subtracted from the band selection, and the ratio of the band selection to the liver control was calculated for every band for each blot separately. Analysis was performed using Microsoft Excel, and expression values were compared between groups (carrier versus noncarrier; and AMD versus non-AMD) using two-sided *t*-tests assuming unequal variances.

ELISA

We developed our ELISA protocol based on previously described methods.³² We tested the accuracy of our assay on normal blood donor plasma from the Hematopoietic Biorepository and Cellular Therapy Shared Resource at Case Western Reserve University in triplicate along with purified CFH and purified liver lysate controls. Our final ELISA protocol involved liver lysate as a standard in dilutions ranging from 1:1 to 1:4096 in serial dilutions for accuracy. Analyses were completed in Microsoft Excel according to standard methods.³⁵ Each incubation was performed on a rocker for maximum efficiency.

We diluted plasma from Amish and non-Amish study participants at 1:4096 in 50 μ L per well in triplicate. Samples were double-blinded from all researchers involved in the analysis and were randomly allocated to each plate regardless of P503A genotype or whether they were AMD-affected or unaffected. All antibodies utilized in this protocol came from Abcam, Cambridge, MA, USA. We first diluted mouse monoclonal anti-CFH (85 ng/mL, ab118820) at 1:500 in 50 μ L per well. Plates were incubated overnight for maximum capture at 4°C. We washed the plates 4 times with PBS and 0.05% TWEEN. We added 100 μ L of blocking solution (1% BSA in PBS) and incubated the plates for 2 hours at room temperature. Doubling dilutions of the standard (liver lysate) and plasma samples were incubated at 50 μ L per well in triplicate overnight at 4°C. We added 50 μ L of the sheep polyclonal anti-CFH detection antibody (1.5 μ L/mL, ab8842) to each well and incubated for 3 hours at room temperature. From this point on, the protocol was carried out in darkness. We performed 4 washes and added the HRP conjugate antibody at 50 μ L (145 ng/mL, ab6747) to the plates. A 30-minute room temperature incubation was performed, and the plates were washed 4 times. We added 100 μ L of chromogen (TMB) and incubated the plates at room temperature for 1 hour. We added 100 μ L of 0.5 M sulfuric acid for the stop solution to end the reaction. Plates were read immediately at 450 nm on the Fluostar machine. Analyses were discrete; however, tests were performed to confirm that 450 nm was the ideal

wavelength to read on the original protocol development plates. Analyses to determine relative CFH protein expression in our assays were performed in Microsoft Excel.

CFH Protein Modeling

To understand the effects of *CFH* P503A on CFH protein structure, we modeled P503 and A503 versions of the amino acid sequence with the Phyre² software program.³⁴ Specifically, we evaluated the amino acid sequence for short consensus repeat (SCR) domain 8 (SCR8) of CFH with and without the amino acid substitution at position 58 in the sequence of 62 amino acids. We used the Chimera software program³⁵ to examine if the amino acid substitution changed the predicted number of contacts between residue 503 and the neighboring residues. Contacts included all types of direct interactions within the protein structure, including polar and nonpolar interactions as well as favorable and unfavorable interactions.

RESULTS

Identification of Additional CFH P503A Carriers in the Amish

We performed genotyping assays (Supplementary Fig. S1) on genomic DNA samples from 1326 Amish individuals (523 from Ohio, 306 from Indiana, and 497 from Pennsylvania) and identified 39 additional carriers of the risk allele for *CFH* P503A. Therefore, in total, we have identified 58 carriers, including 57 heterozygotes and 1 homozygote. Of these 58 carriers, 20 have AMD (8 self-reported and 12 clinically confirmed), 33 do not have AMD (29 clinically confirmed and 4 self-reported), and 5 have an unknown AMD status. Using data from the AGDB, we found that these 58 individuals are related through a 1101-person pedigree that traces back to 12 common ancestors (Fig. 1). All 58 individuals with the risk allele for *CFH* P503A were from Ohio and Indiana.

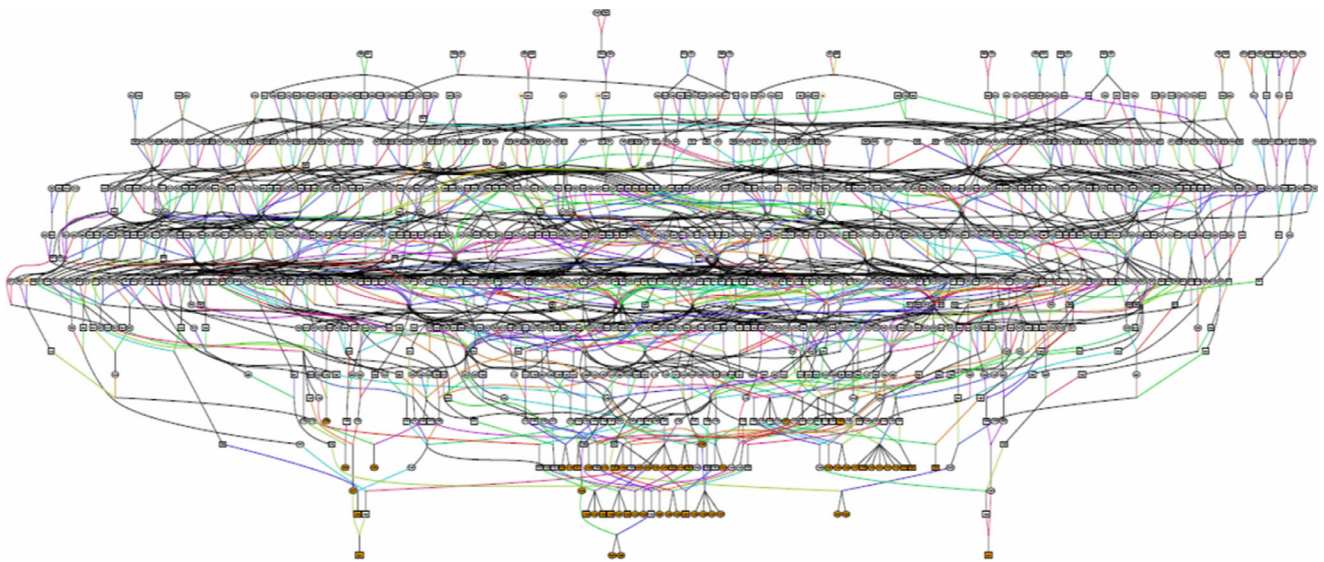


FIGURE 1. All-connecting path pedigree for the 58 Amish individuals with the risk allele for *CFH* P503A. The ancestry of the 58 carriers can be traced to 12 common ancestors (6 married couples). The pedigree was drawn using genealogy information from the AGDB and the Pedigraph software tool. Circles represent women, and squares represent men. Carriers are highlighted in orange.

TABLE. Association Test Results for *CFH* P503A and AMD

Kinship Matrix	Covariate Adjustments	Full Dataset (<i>n</i> = 1065)		Newly Ascertained Dataset Only (<i>n</i> = 1006)	
		Effect Estimate	<i>P</i> Value	Effect Estimate	<i>P</i> Value
ACP	None	0.95	0.009	−0.034	0.94
	Age + sex	0.68	0.08	0.46	0.42
	Age + sex + location	0.57	0.14	0.26	0.64
Sibships	None	0.99	0.004	−0.055	0.90
	Age + sex	0.67	0.06	0.44	0.42
	Age + sex + location	0.53	0.15	0.18	0.72

Effect estimates (betas) and *P* values were calculated using a generalized linear mixed model accounting for kinship information from kinship matrices comprised of the (i) full ACP and (ii) immediate familial relationships of the genotyped individuals alone (i.e. sibships) in the “full dataset,” which included 224 AMD-affected (93 Ohio, 38 Indiana, and 93 Pennsylvania) and 841 unaffected (250 Ohio, 220 Indiana, and 371 Pennsylvania) Amish individuals. Among these 1065 individuals, 59 individuals (12 AMD-affected carriers, 6 unaffected carriers, 15 AMD-affected noncarriers, and 26 unaffected noncarriers) were also part of the *CFH* P503A discovery analyses.¹³ Therefore, we also performed association analyses in the newly ascertained dataset alone, which included 197 AMD-affected (73 Ohio, 31 Indiana, and 93 Pennsylvania) and 809 unaffected (222 Ohio, 216 Indiana, and 371 Pennsylvania) Amish individuals. For both datasets, we considered unadjusted models, models adjusting for age at examination and sex, and models adjusting for age at examination, sex, and location of ascertainment (Ohio, Indiana, and Pennsylvania).

None of the nearly 500 Lancaster County Amish that were genotyped in our study had a copy of this risk allele.

Association Tests

To determine if there is still a statistical association between the risk allele for *CFH* P503A and AMD, we performed association tests in our updated dataset of Amish individuals from Ohio, Indiana, and Pennsylvania with known *CFH* P503A genotype and AMD status. Of the 1065 individuals in our updated dataset (224 AMD-affected and 841 unaffected), 50 were risk allele carriers (49 heterozygous and 1 homozygous; and 18 AMD-affected and 32 unaffected), and 1015 were noncarriers (206 AMD-affected and 809 unaffected). We detected modest association signals in our unadjusted analyses ($P = 0.009$ and 0.004 with ACP-based and sibship-based matrices, respectively); however, including additional covariates to account for age, sex, and the different Amish communities involved in this study (Ohio, Indiana, and Pennsylvania) reduced these association signals (Table).

Because 59 individuals in our association tests were also part of the *CFH* P503A discovery association analyses,¹³ we performed subset analyses using data from only the newly ascertained study participants ($n = 1006$; 197 AMD-affected and 809 unaffected; and 32 heterozygous risk allele carriers and 974 noncarriers) and found that the modest association signals we detected with the full dataset were diminished (see the Table), suggesting the importance of the originally identified risk allele carriers in the association tests.

Age at Diagnosis

To gauge if the individuals with the risk allele for P503A exhibited an earlier age of AMD onset compared to individuals without the risk allele, we compared the age at first AMD diagnosis in carriers and noncarriers of the risk allele. The carriers did not exhibit a significantly earlier age at first AMD diagnosis compared to noncarriers in our Kaplan-Meier survival curve analysis ($P = 0.59$); however, several of the carriers appear to have an earlier age of AMD onset compared to most of the noncarriers (Fig. 2). The average ages at AMD diagnosis were 69.9 and 71.2 years for affected carriers ($n = 7$) and noncarriers ($n = 154$), respec-

tively. These observations were consistent with the results from our pairwise Wilcoxon rank-sum tests between age at AMD diagnosis for carriers and noncarriers (Supplementary Fig. S2).

CFH RNA Quantification and Analysis

To understand the effects of *CFH* P503A on *CFH* gene products, we examined mRNA expression of *CFH* in 40 whole blood samples from *CFH* P503A risk allele carriers and closely related noncarriers. Real-time quantitative PCR was executed with four different TaqMan assays targeting the three protein-coding transcripts of *CFH* (CFH-202, 206, and 201) and the large retained intron of *CFH* (CFH-203). Four samples were removed as outliers from our analysis because their relative expression fell outside 1.5 times the IQR in at least one group (carrier/AMD, carrier/non-AMD, noncarrier/AMD, and noncarrier/non-AMD) of at least one of the

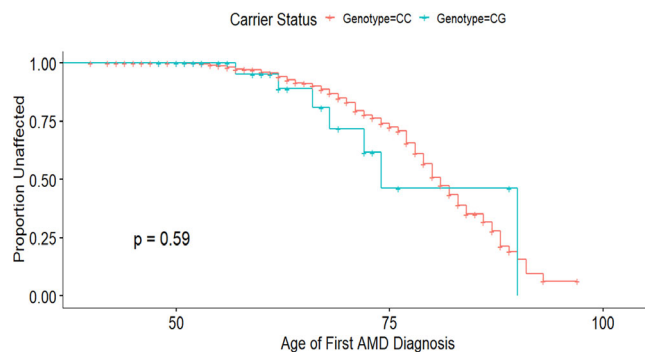


FIGURE 2. Age at AMD diagnosis for carriers and non-carriers of the risk allele for *CFH* P503A. The AMD statuses of 826 Amish individuals were evaluated, including 31 risk allele carriers (7 with AMD and 24 without AMD) and 795 noncarriers (154 with AMD and 641 without AMD) from the Ohio, Indiana, and Pennsylvania Amish populations. Blue represents the risk allele carriers (Genotyped = CG), and red represents the noncarriers (Genotyped = CC). The y-axis depicts the proportion of carriers and noncarriers that were considered unaffected at their eye examination. The x-axis depicts the ages at which individuals received their first diagnosis of AMD based on their eye examination.

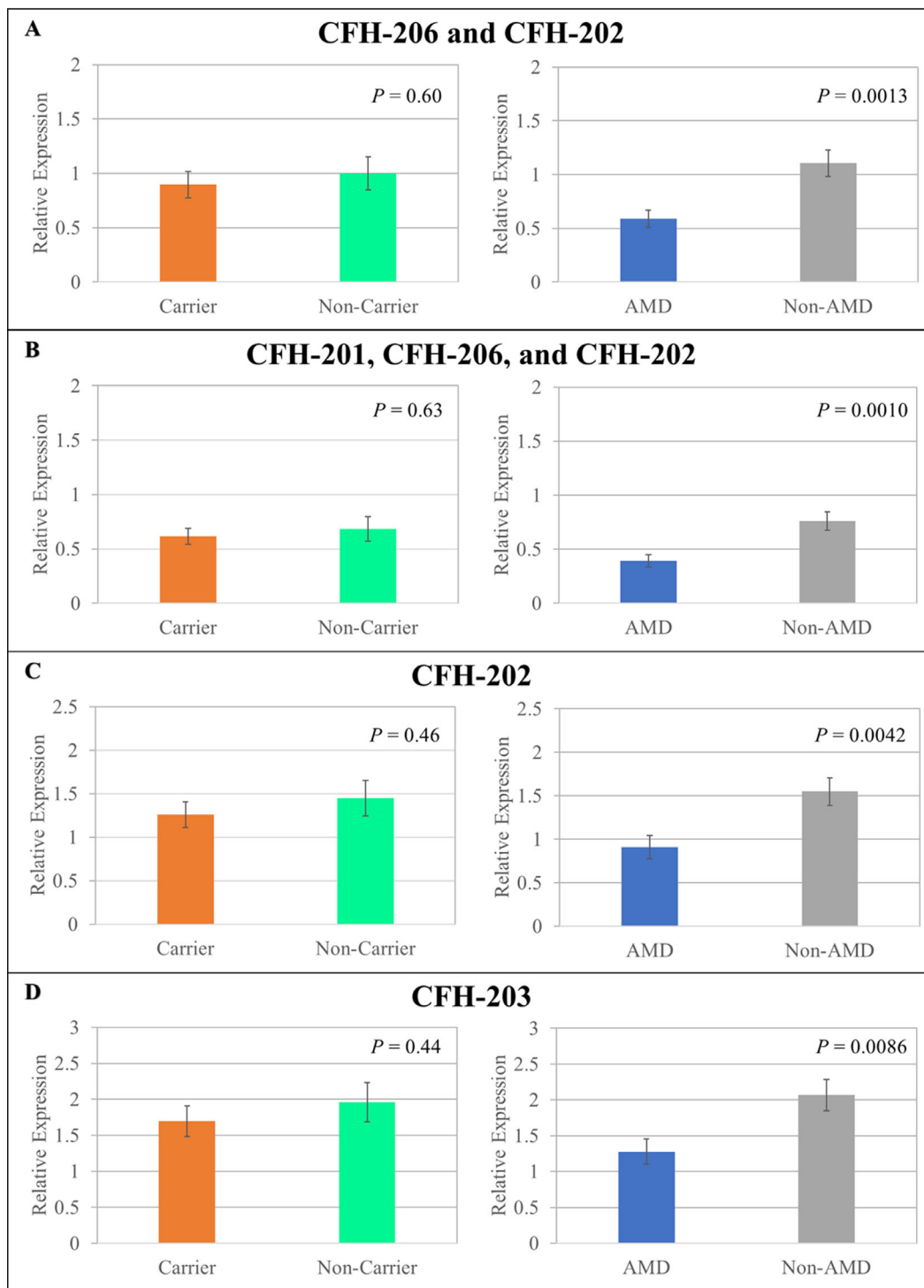


FIGURE 3. Relative expression of *CFH* transcripts in carriers and noncarriers with and without AMD. We measured expression of the following transcripts: (A) CFH-206 and CFH-202; (B) CFH-201, CFH-206, and CFH-202; (C) CFH-202; (D) CFH-203. Four samples were removed as outliers because their relative *CFH* expression levels fell outside 1.5 times the IQR in at least one group of at least one of the assays we performed. This included one affected carrier, two unaffected carriers, and one unaffected noncarrier. Sample sizes for each group: $n = 18$ for carrier; $n = 18$ for noncarrier; $n = 11$ for AMD; and $n = 25$ for non-AMD. Statistical differences among relative *CFH* transcript expression levels from carriers and noncarriers with and without AMD were evaluated using two-sided *t*-tests assuming unequal variance. Error bars represent the standard error of the mean for each group. Assay results shown in panels A and B were normalized to ACTB, and assay results shown in panels C and D were normalized to TBP.

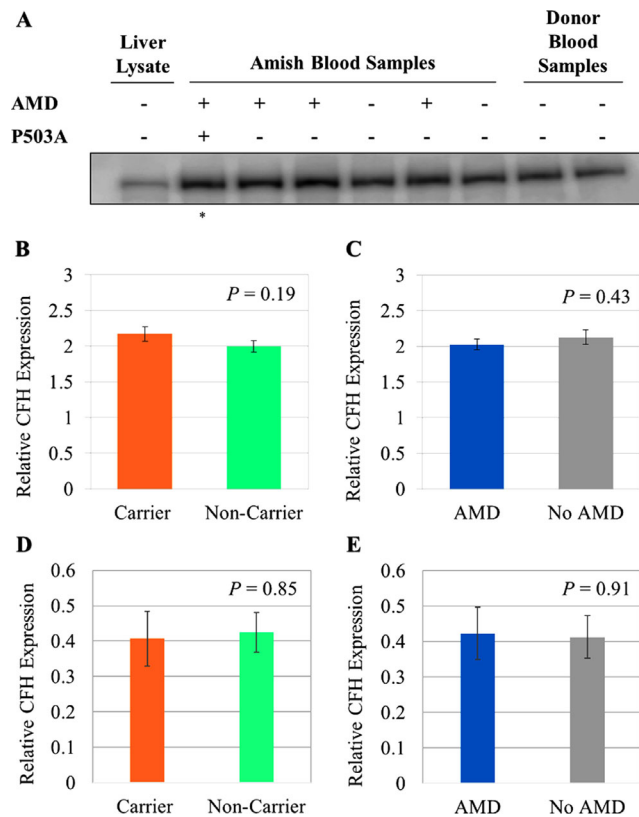


FIGURE 4. CFH protein expression in plasma. (A) Representative Western blot measuring relative CFH protein expression in plasma from carriers (sample from the homozygous risk allele carrier is noted with an asterisk (*); all other carriers are heterozygous for the risk allele) and noncarriers with differing AMD diagnoses. Plasma from normal blood donors and liver CFH lysate were used as controls in our experiments. (B) Comparison of CFH protein expression in plasma from carriers of the risk allele ($n = 38$) versus noncarriers of the risk allele ($n = 43$) measured by 14 Western blots. (C) Comparison of CFH protein expression in plasma from individuals affected by AMD ($n = 39$) versus unaffected individuals ($n = 42$) measured by 14 Western blots. (D) Comparison of CFH protein expression in plasma from carriers of the risk allele ($n = 44$) versus noncarriers of the risk allele ($n = 52$) measured by five ELISA experiments. (E) Comparison of CFH protein expression in plasma from individuals affected by AMD ($n = 40$) versus unaffected individuals ($n = 56$) measured by five ELISA experiments. The P values for all comparisons in panels B to E were calculated using two-sided t -tests assuming unequal variance. Error bars represent the standard error of the mean for each group.

4 assays we performed in this study: 1 affected carrier, 2 unaffected carriers, and 1 unaffected noncarrier. The P503A variant falls within the following transcripts: CFH-202 and CFH-203. We did not observe significant differences in relative CFH levels in any of the assays we performed based on CFH risk allele status alone (Fig. 3). However, there were significant differences ($P < 0.05$) in expression levels in all four assays when comparing blood samples from AMD-affected versus unaffected Amish individuals (see Fig. 3).

The combined relative expression of the CFH-206 and 202 transcripts was significantly higher in the noncarriers without AMD compared to the affected noncarriers (Supplementary Fig. S4A). The combined relative expression of the three protein-coding transcripts of CFH (CFH-201, 206, and 202) was significantly higher in the carriers and noncarriers with-

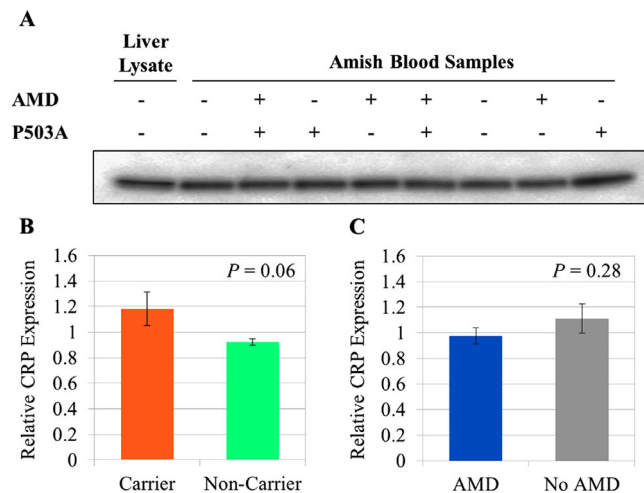


FIGURE 5. CRP protein expression in plasma. (A) Representative Western blot measuring relative CRP expression in plasma from heterozygous carriers and noncarriers with differing AMD diagnoses. Liver CRP lysate was used as a control in our experiments. (B) Comparison of CRP expression in plasma from carriers of the risk allele ($n = 37$) versus noncarriers of the risk allele ($n = 41$) measured by 10 Western blots. (C) Comparison of CRP expression in plasma from individuals affected by AMD ($n = 37$) versus unaffected individuals ($n = 41$) measured by 10 Western blots. The P values for all comparisons in panels B and C were calculated using two-sided t -tests assuming unequal variance. Error bars represent the standard error of the mean for each group.

out AMD compared to the affected noncarriers (Supplementary Fig. S4B). Relative expression of CFH-202 was significantly higher in the carriers and noncarriers without AMD compared to the affected noncarriers (Supplementary Fig. S4C). There were no significant differences among groups for the relative expression of CFH-203 (Supplementary Fig. S4D).

CFH Protein Expression

To observe if the risk allele for CFH P503A affects CFH protein expression, we performed Western blot analyses and ELISA assays with plasma from carriers and noncarriers who were affected or unaffected by AMD. In our samples, we did not identify strong changes to CFH expression based on P503A carrier status or AMD status (Fig. 4). Plasma from the homozygous carrier did not have a marked change in CFH expression compared to the other individuals' samples we assayed (see lane 2 in Fig. 4A).

CRP Protein Expression

To elucidate if CFH P503A alters CRP expression, we carried out Western blot analyses with plasma from carriers and noncarriers with differing AMD diagnoses (Fig. 5). We observed higher relative CRP expression in carriers of the risk allele compared to noncarriers, but this difference was not statistically significant ($P = 0.06$; see Fig. 5B). Similarly, individuals without AMD had slightly higher relative CRP expression compared to AMD-affected individuals, but this difference was not statistically significant ($P = 0.28$; see Fig. 5C).

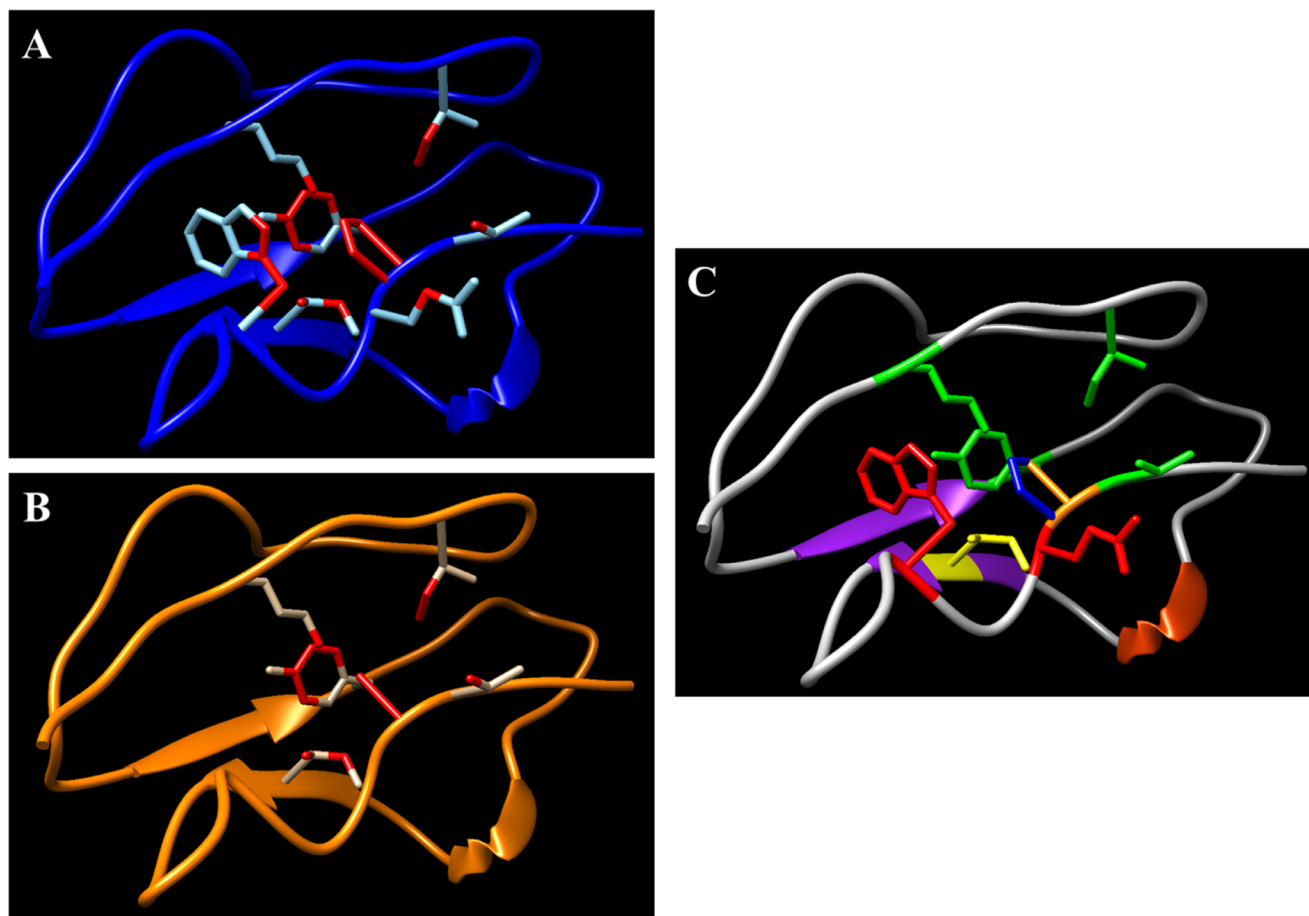


FIGURE 6. Visualization of protein models containing the amino acid substitution for *CFH* P503A in SCR8 domain of *CFH*. Models were visualized with Chimera software.³⁵ (A) SCR8 with P503 and interacting residues. Points of contact are depicted in red. (B) SCR8 with A503 and interacting residues. Points of contact are depicted in red. (C) Superposition of P503 (blue residue) and A503 (orange residue) protein models and neighboring contacts. Residues colored in green maintained the same contacts in the P503 and A503 structures. Red residues lost contact with A503 that interacted with P503. The yellow residue had reduced contacts with A503 compared to P503.

Protein Modeling

Because the risk allele of *CFH* P503A results in an amino acid substitution of a proline for an alanine, we computationally investigated if this substitution yielded any structural changes to the *CFH* protein. In the risk-associated version of the structure (A503), there were fewer contacts between the amino acid at position 503 and the nearby residues when we modeled the domain (SCR8) in which the variant occurs (Fig. 6). Specifically, there were 21 contacts predicted in Chimera for the P503 structure, and there were only 12 contacts predicted between A503 and neighboring residues. Although contacts with three neighboring residues (I455, Y475, K450, and T504) remained consistent between models, there were no contacts between two residues (W499 and Q502) and A503 and reduced contacts between one residue (I492) and A503 compared to P503 (Fig. 6).

DISCUSSION

In this study, we aimed to characterize the effects of *CFH* P503A in the Amish population. All 58 individuals with the risk allele were from Ohio and Indiana Amish commu-

nities. We failed to find any Amish individuals from our Lancaster County Amish cohort with the risk allele for *CFH* P503A. Therefore, we hypothesize that this risk allele segregated within the Midwest Amish subpopulation because of the second Amish migration in the United States in the 1800s. The Lancaster County Amish and the Midwest Amish communities are distinct as evidenced by differences in family surnames and settlement timelines; therefore, it is unsurprising that they could differ genetically as well.²³ Using data from the Swiss Anabaptist Genealogical Association, we determined that the 12 common ancestors of the 58 carriers were from Europe as well as Berks and Somerset Counties in Pennsylvania (Supplementary Fig. S3).

Although this variant was initially identified in the Amish communities of Ohio and Indiana in the United States, other studies have identified heterozygous individuals for *CFH* P503A, including the DiscovEHR,³⁶ TOPMed,³⁷ and gnomAD³⁸ databases. In each of these databases, there are no more than 10 individuals with the risk allele. It is unclear if the individuals in the DiscovEHR study are heterozygous or homozygous, but the allele frequency of *CFH* P503A was less than 0.001.³⁶ The DiscovEHR browser was created from a collaboration between the Geisinger Health System

and Regeneron Genetics Center.³⁶ The study participants were originally recruited through the MyCode Community Health Initiative, which enrolled patients from Geisinger clinics in central and northeastern Pennsylvania.³⁹ Pennsylvania has among the highest populations of Amish individuals in North America²⁴; therefore, it is possible that some of these carriers in the DiscovEHR study are Amish or of Amish descent.

TOPMed (<https://bravo.sph.umich.edu/freeze8/hg38/variant/snv/1-196713905-C-G>) and gnomAD (<https://gnomad.broadinstitute.org/variant/1-196683035-C-G>) only have heterozygous *CFH* P503A carriers. In TOPMed Freeze8, there are five heterozygotes for the risk allele. The six heterozygotes in gnomAD (version 2.1.1, non-TOPMed) are between 60 and 65 years old, which is the age at which some people begin to develop AMD.^{18,40} The individuals with the risk allele for *CFH* P503A in gnomAD are from the following ancestries: African, north-western European, and other non-Finnish European. In the AMD literature, two studies identified AMD-affected individuals with one copy of the risk allele. In one study, a heterozygote for *CFH* P503A was identified among AMD cases from an aggregated dataset of individuals from Radboud University Medical Center in the Netherlands and the European Genetic Database (EUGENDA).⁴¹ Similarly, one heterozygote with AMD was identified in a dataset that included study participants from Boston, France, and Baltimore.⁴² As described, it is unclear which geographic region this individual is from in this study. Despite this, the identification of carriers in these other datasets suggests that the risk allele for *CFH* P503A is not Amish-specific.

CFH P503A was previously identified as an AMD risk variant in the Amish ($P = 9.27 \times 10^{-13}$) using the MQLS software⁴³ on data from 95 AMD-affected, 653 unaffected, and 225 unknown AMD status individuals.¹³ The risk allele was present in 19 Amish individuals (1 homozygous for the risk allele and 18 heterozygotes).¹³ Notably, the MQLS method used in that study allowed for the inclusion of individuals of unknown phenotype and genotype but known familial relatedness to others in the analysis through a complex 13-generation pedigree, but it did not allow for the inclusion of covariates, like age at AMD diagnosis, in the association test.⁴³ By contrast, in our study, we used generalized linear mixed models accounting for familial relatedness (through immediate sibships or the full ACP) and covariates (age, sex, and Amish community location) in individuals with only known AMD statuses (224 AMD-affected and 841 unaffected; see the Table). Among these 1065 individuals, there were 50 risk allele carriers (49 heterozygous and 1 homozygous; and 18 AMD-affected and 32 unaffected) and 1015 noncarriers (206 AMD-affected and 809 unaffected). Although we observed modest association signals in our unadjusted analyses, these signals diminished when we adjusted for covariates (age, sex, and location; see the Table). These signals were also diminished in our subset analyses in which we excluded any individuals who were part of the *CFH* P503A discovery analyses (see the Table). This suggested the importance of the originally identified risk carriers in the association tests, including the only homozygous individual for the risk allele. Whereas previous work suggested that analyzing data with unknown population structure could result in inflated type 1 error, it was also reported that MQLS was considered the most powerful when the pedigree structure is known,⁴⁴ and our subsequent MQLS tests on simulated complex pedigree data showed that the type 1 error rate was

not inflated.⁴⁵ However, because covariates were not considered in these previous studies, it is unknown how MQLS tests including individuals of unknown phenotype and/or genotype status would perform in covariate-adjusted analyses. Therefore, additional research is needed to parse out the roles of using data from (i) individuals of unknown phenotype and/or genotype status but known familial relatedness and (ii) different covariates in highly inter-related family-based association studies.

The P503A variant is about 15 bp from the end of exon 10 in the *CFH* gene. Using the Human Splicing Finder version 3 (<http://www.umd.be/HSF3/>), we found that the risk allele appears to break an exonic splicing enhancer (ESE) site, which may alter splicing of *CFH*. We interrogated if the risk allele for *CFH* P503A alters expression of any of the *CFH* transcripts. The variant falls within the full-length protein-coding transcript of *CFH* (CFH-202) and the retained intron transcript (CFH-203) but does not lead to significant changes in expression of these transcripts in the blood. Although relative *CFH* expression varied significantly between some groups in our assays, carrier status alone could not explain these differences (see Fig. 3; Supplementary Fig. S4). In contrast, other rare *CFH* variants (chr1:196648924G>A and chr1:196642295T>C) located in splice sites lead to reduced serum CFH protein levels in carriers of the risk allele.^{42,46} Other studies have shown that transcript levels of *CFH* in the RPE-choroid are not significantly different among AMD cases and controls^{15,47} or among Y402H carriers and noncarriers.⁴⁷ Additionally, individuals with the risk allele for P503A were not significantly younger at their first AMD diagnoses compared to homozygotes for the non-risk allele. This is in contrast with carriers of another rare *CFH* variant (R1210C), which experienced AMD symptoms at significantly younger ages than noncarriers did.¹²

We interrogated CFH protein expression in plasma samples from Amish individuals with and without the risk allele for *CFH* P503A. We hypothesized that *CFH* P503A causes misfolding of the protein which would be degraded through the unfolded protein response and result in lower CFH expression in carriers compared to noncarriers. However, our data suggest that the risk allele does not noticeably affect CFH protein expression in these individuals. The lack of an effect on CFH protein abundance has been similarly observed for other missense risk alleles in *CFH* for AMD, including the common, high-effect variant (Y402H, rs1061170) that has been repeatedly associated with AMD. Additionally, significant differences in systemic CFH levels have not been observed between plasma and serum samples from AMD cases and controls in independent cohorts.⁴⁸ Rather than affecting protein expression of CFH, the Y402H variant affects the binding of CFH to its ligands including heparin and CRP.⁴⁹ Y402H also lowers the binding affinity of plasma CFH to oxidized low-density lipoprotein (oxLDL), which may influence systemic and local oxidative stress.⁵⁰ On the other hand, the protective AMD variant in *CFH* (I62) contributes to increased binding of the CFH protein to C3b in the complement pathway.⁵¹

The *CFH* P503A variant is a missense mutation that results in the conversion of a proline residue to an alanine residue in a domain of the CFH protein that contains binding sites for C3b, CRP, and cell surface proteins of pathogenic bacteria which recruit CFH to prevent complement attack.⁵² Therefore, this variant may alter the binding affinities of CFH for some of its ligands in the complement cascade.

Our protein modeling suggests that modest conformational changes occur in SCR8 of CFH due to P503A. Therefore, further investigation of the binding capabilities of CFH P503 and A503 need to be performed.

Although we observed that P503A status did not affect CFH expression levels, this does not eliminate the possibility that it is impeding CFH function, which may be more aptly observed by examining its effects on other members of the complement pathway. Eyes of deceased study participants who were homozygous for *CFH* Y402H have elevated levels of C5a, IL-18, and TNF- α that may lead to heightened activity of the complement and NF- κ B pathways.⁵³ Carriers of the risk allele for Y402H also have higher CRP expression in the RPE-choroid.⁴⁷ Although our data suggest that systemic CRP levels measured in plasma did not differ significantly in carriers and noncarriers, we did not investigate local changes to CRP levels in human eye tissue. Plasma samples from individuals with exudative AMD have higher CRP levels than samples from controls, independent of *ARMS2* and *CFH* genotype status.⁵⁴ Therefore, investigations of other members and ligands of the complement pathway should be performed for *CFH* P503A to determine if there are broader effects of the risk allele independent of CFH expression.

Although we interrogated the effects of *CFH* P503A in blood samples from Amish carriers and noncarriers of the risk allele, we were unable to assess these potential consequences in eye tissue. Due to their cultural beliefs, we are unable to acquire eye tissue from Amish study participants. As with other studies that examine the effects of *CFH* variants in the blood, our approach to study *CFH* P503A in the blood begins to interrogate the role of this variant in systemic complement activity. However, its effects may be different in the eyes due to tissue-specific effects and ocular immune privilege.⁵⁵ CFH is predominantly synthesized in the liver and secreted into the bloodstream to circulate throughout the body.⁵⁶ CFH is also constitutively expressed by RPE cells in the human eyes and protects these cells from complement attack.⁵⁷ Perturbations in CFH are suspected to alter both systemic and local complement regulation and promote immune responses in the retina that contribute to AMD.^{18–20} Therefore, the potential consequences of *CFH* P503A on local complement activity need to be explored. Additionally, although we have identified the highest number of carriers of the risk allele for *CFH* P503A in a single cohort, we are limited by the small number of carriers ($n = 57$ heterozygotes and $n = 1$ homozygote) in our functional experiments and statistical analyses. Consequently, we were underpowered (power < 0.80) to detect small to modest effects of risk allele carrier status on *CFH* RNA expression as well as CFH and CRP levels (Supplementary Table S1).

In this study, we characterized the effects of a rare, missense variant (*CFH* P503A) for AMD in Amish individuals. We did not observe significant differences in mRNA and protein expression of CFH in Amish blood samples from carriers and noncarriers of the risk allele. However, the substitution of an alanine amino acid for a proline amino acid at position 503 appears to change the number of contacts among neighboring residues in SCR8 of CFH. Therefore, this variant may affect binding affinities for ligands of CFH and other members of the complement pathway, and additional research is required to confirm this hypothesis. Elucidating the impacts of risk variants, like *CFH* P503A, on both local and systemic complement activity could lead

to new knowledge of the pathophysiology of AMD and promote the creation of novel therapeutics.

Acknowledgments

The authors thank the Amish community members for participating in this study. This work made use of the Anabaptist Genealogy Database (AGDB) and genealogy data curated by the Swiss Anabaptist Genealogical Association. This work made use of the High Performance Computing Resource in the Core Facility for Advanced Research Computing at Case Western Reserve University as well as resources from the Visual Sciences Research Center at Case Western Reserve University.

Supported by the National Institutes of Health (NIH; EY023164). M.G. was supported by a postdoctoral NIH Visual Sciences Training Program (T32EY007157-18). A.R.W. was supported by the CWRU Visual Sciences Training Program (T32 EY 7157-19) and the Clinical and Translational Science Collaborative (CTSC) of Cleveland which is funded by the National Institutes of Health (NIH), National Center for Advancing Translational Science (NCATS), Clinical and Translational Science Award (CTSA) grant (TL1TR002549). The content is solely the responsibility of the authors and do not necessarily represent the official views of the NIH.

Disclosure: **A.R. Waksmunski**, None; **K. Miskimen**, None; **Y.E. Song**, None; **M. Grunin**, None; **R. Laux**, None; **D. Fuzzell**, None; **S. Fuzzell**, None; **L.D. Adams**, None; **L. Caywood**, None; **M. Prough**, None; **D. Stambolian**, None; **W.K. Scott**, None; **M.A. Pericak-Vance**, None; **J.L. Haines**, None

References

- Flaxel CJ, Adelman RA, Bailey ST, et al. Age-Related Macular Degeneration Preferred Practice Pattern(R). *Ophthalmology*. 2020;127(1):P1–P65.
- Mitchell P, Liew G, Gopinath B, Wong TY. Age-related macular degeneration. *Lancet*. 2018;392(10153):1147–1159.
- Seddon JM, Ajani UA, Mitchell BD. Familial Aggregation of Age-related Maculopathy. *Am J Ophthalmol*. 1997;123(2):199–206.
- De Jong PTVM, Klaver CCW, Wolfs RCW, Assink JJM, Hofman A. Familial Aggregation of Age-related Maculopathy. *Am J Ophthalmol*. 1997;124(6):862.
- Klaver CC, Wolfs RC, Assink JJ, van Duijn CM, Hofman A, de Jong PT. Genetic risk of age-related maculopathy. Population-based familial aggregation study. *Arch Ophthalmol*. 1998;116(12):1646–1651.
- Klein ML, Mauldin WM, Stoumbos VD. Heredity and age-related macular degeneration. Observations in monozygotic twins. *Arch Ophthalmol*. 1994;112(7):932–937.
- Meyers SM, Greene T, Gutman FA. A Twin Study of Age-related Macular Degeneration. *Am J Ophthalmol*. 1995;120(6):757–766.
- Hammond CJ, Webster AR, Snieder H, Bird AC, Gilbert CE, Spector TD. Genetic influence on early age-related maculopathy: a twin study. *Ophthalmology*. 2002;109(4):730–736.
- Seddon JM, Cote J, Page WF, Aggen SH, MC Neale. The US twin study of age-related macular degeneration: relative roles of genetic and environmental influences. *Arch Ophthalmol*. 2005;123(3):321–327.
- Seddon JM, George S, Rosner B. Cigarette smoking, fish consumption, omega-3 fatty acid intake, and associations with age-related macular degeneration: the US Twin Study of Age-Related Macular Degeneration. *Arch Ophthalmol*. 2006;124(7):995–1001.

11. Fritsche LG, Igl W, Cooke Bailey JN, et al. A large genome-wide association study of age-related macular degeneration highlights contributions of rare and common variants. *Nat Genet.* 2016;48(2):134–143.
12. Raychaudhuri S, Iartchouk O, Chin K, et al. A rare penetrant mutation in CFH confers high risk of age-related macular degeneration. *Nat Genet.* 2011;43(12):1232–1236.
13. Hoffman JD, Cooke Bailey JN, D'Aoust L, et al. Rare complement factor H variant associated with age-related macular degeneration in the Amish. *Invest Ophthalmol Vis Sci.* 2014;55(7):4455–4460.
14. Waksmunski AR, Igo RP, Jr., Song YE, et al. Rare variants and loci for age-related macular degeneration in the Ohio and Indiana Amish. *Hum Genet.* 2019;138(10):1171–1182.
15. Hageman GS, Anderson DH, Johnson LV, et al. A common haplotype in the complement regulatory gene factor H (HF1/CFH) predisposes individuals to age-related macular degeneration. *Proc Natl Acad Sci U S A.* 2005;102(20):7227–7232.
16. Haines JL, Hauser MA, Schmidt S, et al. Complement factor H variant increases the risk of age-related macular degeneration. *Science.* 2005;308(5720):419–421.
17. Klein RJ, Zeiss C, Chew EY, et al. Complement factor H polymorphism in age-related macular degeneration. *Science.* 2005;308(5720):385–389.
18. Ayoub T, Patel N. Age-related macular degeneration. *J R Soc Med.* 2009;102(2):56–61.
19. Warwick A, Khandhadia S, Ennis S, Lotery A. Age-Related Macular Degeneration: A Disease of Systemic or Local Complement Dysregulation? *J Clin Med.* 2014;3(4):1234–1257.
20. Scholl HP, Charbel Issa P, Walier M, et al. Systemic complement activation in age-related macular degeneration. *PLoS One.* 2008;3(7):e2593.
21. Cooke Bailey JN, Sobrin L, Pericak-Vance MA, Haines JL, Hammond CJ, Wiggs JL. Advances in the genomics of common eye diseases. *Hum Mol Genet.* 2013;22(R1):R59–R65.
22. Weber BH, Charbel Issa P, Pauly D, Herrmann P, Grassmann F, Holz FG. The role of the complement system in age-related macular degeneration. *Dtsch Arztebl Int.* 2014;111(8):133–138.
23. McKusick VA, Hostetler JA, Egeland JA. Genetic studies of the Amish, background and potentialities. *Bulletin of the Johns Hopkins Hospital.* 1964;115:203–222.
24. Nittala MG, Song YE, Sardell R, et al. AMISH EYE STUDY: Baseline Spectral Domain Optical Coherence Tomography Characteristics of Age-Related Macular Degeneration. *Retina.* 2019;39(8):1540–1550.
25. Seddon JM, Sharma S, Adelman RA. Evaluation of the clinical age-related maculopathy staging system. *Ophthalmology.* 2006;113(2):260–266.
26. Sardell RJ, Nittala MG, Adams LD, et al. Heritability of Choroidal Thickness in the Amish. *Ophthalmology.* 2016;123(12):2537–2544.
27. Agarwala R, Biesecker LG, Schaffer AA. Anabaptist genealogy database. *Am J Med Genet C Semin Med Genet.* 2003;121C(1):32–37.
28. Garbe JR, Da Y. Pedigraph: A Software Tool for the Graphing and Analysis of Large Complex Pedigree. 2008; User manual Version 2.4. Available from: https://animalgene.umn.edu/sites/animalgene.umn.edu/files/pedigraph_manual.pdf.
29. Sinnwell JP, Therneau TM, Schaid DJ. The kinship2 R package for pedigree data. *Hum Hered.* 2014;78(2):91–93.
30. Schneider CA, Rasband WS, Eliceiri KW. NIH Image to ImageJ: 25 years of image analysis. *Nat Methods.* 2012;9(7):671–675.
31. Davarinejad H. Quantifications of western blots with Image J 2017. Available from: <http://www.yorku.ca/yisheng/Internal/Protocols/ImageJ.pdf>.
32. Ansari M, McKeigue PM, Skerka C, et al. Genetic influences on plasma CFH and CFHR1 concentrations and their role in susceptibility to age-related macular degeneration. *Hum Mol Genet.* 2013;22(23):4857–4869.
33. Grunin M, Burstyn-Cohen T, Hagbi-Levi S, Peled A, Chowers I. Chemokine receptor expression in peripheral blood monocytes from patients with neovascular age-related macular degeneration. *Invest Ophthalmol Vis Sci.* 2012;53(9):5292–5300.
34. Kelley LA, Mezulis S, Yates CM, Wass MN, Sternberg MJ. The Phyre2 web portal for protein modeling, prediction and analysis. *Nat Protoc.* 2015;10(6):845–858.
35. Pettersen EF, Goddard TD, Huang CC, et al. UCSF Chimera—a visualization system for exploratory research and analysis. *J Comput Chem.* 2004;25(13):1605–1612.
36. Dewey FE, Murray MF, Overton JD, et al. Distribution and clinical impact of functional variants in 50,726 whole-exome sequences from the DiscovEHR study. *Science.* 2016;354(6319):aaf6814.
37. Bravo variant browser. Available at: <https://bravo.sph.umich.edu/freeze5/hg38/2018>.
38. Karczewski KJ, Francioli LC, Tiao G, et al. The mutational constraint spectrum quantified from variation in 141,456 humans. *Nature.* 2020;581(7809):434–443.
39. Carey DJ, Fetterolf SN, Davis FD, et al. The Geisinger MyCode community health initiative: an electronic health record-linked biobank for precision medicine research. *Genet Med.* 2016;18(9):906–913.
40. Levine JA, Schmier JK. Economic Impact of Progression of Age-related Macular Degeneration. *US Ophthalmic Review.* 2013;06(01):52.
41. Kersten E, Geerlings MJ, den Hollander AI, et al. Phenotype Characteristics of Patients With Age-Related Macular Degeneration Carrying a Rare Variant in the Complement Factor H Gene. *JAMA Ophthalmol.* 2017;135(10):1037–1044.
42. Triebwasser MP, Roberson ED, Yu Y, et al. Rare Variants in the Functional Domains of Complement Factor H Are Associated With Age-Related Macular Degeneration. *Invest Ophthalmol Vis Sci.* 2015;56(11):6873–6888.
43. Thornton T, McPeck MS. Case-control association testing with related individuals: a more powerful quasi-likelihood score test. *Am J Hum Genet.* 2007;81(2):321–337.
44. Thornton T, McPeck MS. ROADTRIPS: case-control association testing with partially or completely unknown population and pedigree structure. *Am J Hum Genet.* 2010;86(2):172–184.
45. Cummings AC, Torstenson E, Davis MF, et al. Evaluating power and type 1 error in large pedigree analyses of binary traits. *PLoS One.* 2013;8(5):e62615.
46. Wagner EK, Raychaudhuri S, Villalonga MB, et al. Mapping rare, deleterious mutations in Factor H: Association with early onset, drusen burden, and lower antigenic levels in familial AMD. *Sci Rep.* 2016;6:31531.
47. Johnson PT, Betts KE, Radeke MJ, Hageman GS, Anderson DH, Johnson LV. Individuals homozygous for the age-related macular degeneration risk-conferring variant of complement factor H have elevated levels of CRP in the choroid. *Proc Natl Acad Sci U S A.* 2006;103(46):17456–17461.
48. Cipriani V, Lores-Motta L, He F, et al. Increased circulating levels of Factor H-Related Protein 4 are strongly associated with age-related macular degeneration. *Nat Commun.* 2020;11(1):778.

49. Ferreira VP, Pangburn MK, Cortes C. Complement control protein factor H: the good, the bad, and the inadequate. *Mol Immunol*. 2010;47(13):2187–2197.
50. Shaw PX, Zhang L, Zhang M, et al. Complement factor H genotypes impact risk of age-related macular degeneration by interaction with oxidized phospholipids. *Proc Natl Acad Sci U S A*. 2012;109(34):13757–13762.
51. Tortajada A, Montes T, Martinez-Barricarte R, Morgan BP, Harris CL, de Cordoba SR. The disease-protective complement factor H allotypic variant Ile62 shows increased binding affinity for C3b and enhanced cofactor activity. *Human Molec Genetics*. 2009;18(18):3452–3461.
52. Yu J, Wiita P, Kawaguchi R, et al. Biochemical analysis of a common human polymorphism associated with age-related macular degeneration. *Biochemistry*. 2007;46(28):8451–8461.
53. Cao S, Wang JC, Gao J, et al. CFH Y402H polymorphism and the complement activation product C5a: effects on NF-kappaB activation and inflammasome gene regulation. *Br J Ophthalmol*. 2016;100(5):713–718.
54. Shijo T, Sakurada Y, Fukuda Y, et al. Association of CRP levels with ARMS2 and CFH variants in age-related macular degeneration. *Int Ophthalmol*. 2020;40(10):2735–2742.
55. Zhou R, Caspi RR. Ocular immune privilege. *F1000 Biol Rep*. 2010;2:3.
56. Anderson DH, Radeke MJ, Gallo NB, et al. The pivotal role of the complement system in aging and age-related macular degeneration: hypothesis re-visited. *Prog Retin Eye Res*. 2010;29(2):95–112.
57. McHarg S, Clark SJ, Day AJ, Bishop PN. Age-related macular degeneration and the role of the complement system. *Mol Immunol*. 2015;67(1):43–50.